Electronic Supplementary Material (ESI) for Analyst.

Supplementary information:

An FcεRI-IgE-based genetically encoded microfluidic cell sensor for fast gram-negative bacterial screening in food samples

Hui Jiang[a, b], Jun Yang[b], Donglei Jiang[c], Xiulan Sun[*a]

[a] *State Key Laboratory of Food Science and Technology, School of Food Science and Technology, National Engineering Research Center for Functional Food, Synergetic Innovation Center of Food Safety and Nutrition, Jiangnan University, Wuxi, Jiangsu 214122, China*

[b] *Nanjing Institute for Food and Drug Control , Nanjing, Jiangsu 211198, PR China*

[c] *College of Food Science and Engineering, Nanjing University of Finance and Economics, Collaborative Innovation Center for Modern Grain Circulation and Safety, Key Laboratory of Grains and Oils Quality Control and Processing, Nanjing, Jiangsu 210023, PR China*

*Corresponding author.
E-mail address: sxlzyz@jiangnan.edu.cn (Xiulan Sun)

Figures Caption:

Fig. S1. Target sequence design of recombinant protein CD14(Rat)-Fcε IgE.

Fig. S2. (A) Plasmid profile. (B) Agarose gel electrophoresis analysis of CD14(Rat)-IgE Fc plasmid. Lane M: DNA marker；Lane 1: Plasmid of transfection level.

Fig. S3. (A) Identification of protein expression. Lane 1：DMEM of control；Lane 2：DMEM of CD14-Fcε；Lane M1：SDS-PAGE Marker. (B) SDS-PAGE of affinity purification. Lane M：SDS-PAGE Marker；Lane 1：Supernatant after centrifugation；Lane 2：Effluent after supernatant incubating with Ni-IDA；Lane3-6：Elution fractions. (C) SDS-PAGE and Western Blot. Left：SDS-PAGE. Right：Western Blot (using anti-His tag antibody). Lane 1：BSA (1.0 μg)；Lane 2：CD14-Fcε protein (1.2 μg)(Reduced)；Lane 3：CD14-Fcε protein (1.2 μg)(Non-Reduced)；Lane M1: SDS-PAGE Marker；Lane M2: Western Blot Marker.

Fig. S4. Standard curve of protein quantification using BCA.

Fig. S5. Immunofluorescence images of CD14-Fcε bound to *E. coli* ATCC 25922. The bacteria were heat-killed and then incubated with (A) or without (B) CD14-Fcε (6 μg/mL) followed by anti-CD14 (2 μg/mL) and IgG-FITC.

Fig. S6. Plasmid profile of pLenti-CMV-GCaMP6(s)-2A-Tdtomato

Fig. S7. Lentiviral vector transfection and selection of stable transfection cell lines.

Fig. S8. Cell viability and fluorescence efficiency.

Fig. S9. Fluorescence images of stable transfection RBL-2H3 cell lines after A23187 stimulation.

Fig. S10. *β*-hexosaminidase assay for confirmation of RBL-2H3 cells activated by *E.coli* ATCC 25922.

Table S1 Comparison of other methods for bacteria detection.

Target protein sequence:

CD14(Rat)-IgE Fc protein Length=604 MW=66008.8 pI=6.78

```
1     SPATPEPCEL DQDEESVRCY CNFSDPQPNW SSAFLCAGAE DVEFYGGGRS LEYLLKRVDT
61    EANLGQYTDI IRSLPLKRLT VRSARVPTQI LFGTLRVLGY SGLRELTLEN LEVTGTALSP
121   LLDATGPDLN TLSLRNVSWA TTDTWLAELQ QWLKPGLKVL SIAQAHSLNF SCKQVGVFPA
181   LATLDLSDNP ELGEKGLISA LCPHKFPTLQ VLALRNAGME TTSGVCSALA AARVPLQALD
241   LSHNSLRDTA GTPSCDWPSQ LNSLNLSFTG LEHVPKGLPA KLSVLDLSYN RLDRKPRPEE
301   LPEVGSLSLT GNPFLHSESQ SEAYNSGVVI ATALSPGSAG LSGTLALLLG HRLFVHHHHH
361   HGGGGSGGGG SGGGGSDDEP RGVITYLIPP SPLDLYENGT PKLTCLVLDL ESEENITVTW
421   VRERKKSIGS ASQRSTKHHN ATTSITSILP VDAKDWIEGE GYQCRVDHPH FPKPIVRSIT
481   KAPGKRSAPE VYVFLPPEEE EKDKRTLTCL IQNFFPEDIS VQWLQDSKLI PKSQHSTTTP
541   LKYNGSNQRF FIFSRLEVTK ALWTQTKQFT CRVIHEALRE PRKLERTISK SLGNTSLRPS
601   QASM
```

(CD14(Rat) +His +Linker+IgE Fc(CH3+CH4))

Fig. S1. Target sequence design of recombinant protein CD14(Rat)-Fcε IgE.

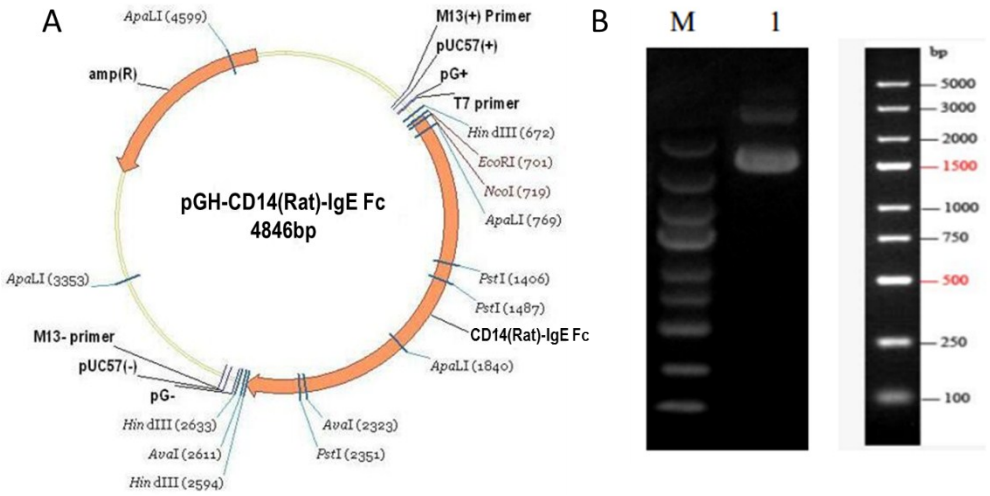

Fig. S2. (A) Plasmid profile. (B) Agarose gel electrophoresis analysis of CD14(Rat)-IgE Fc plasmid. Lane M: DNA marker； Lane 1: Plasmid of transfection level.

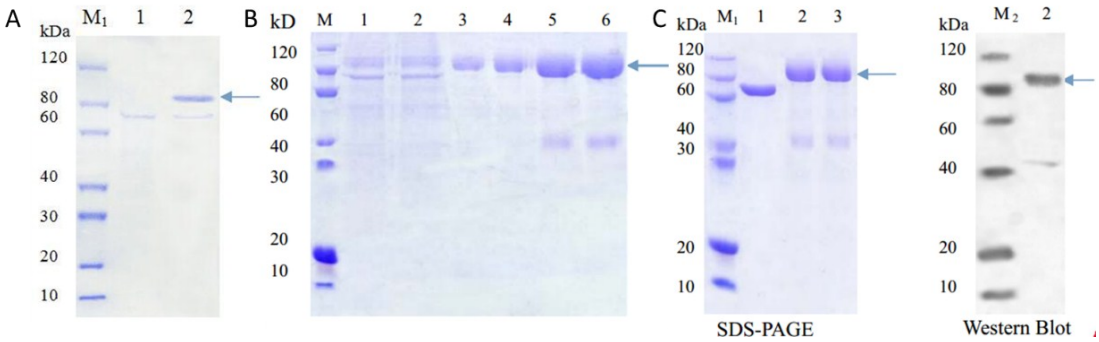

Fig. S3. (A) Identification of protein expression. Lane 1：DMEM of control；Lane 2：DMEM of CD14-Fcε；Lane M1：SDS-PAGE Marker. (B) SDS-PAGE of affinity purification. Lane M：SDS-PAGE Marker；Lane 1：Supernatant after centrifugation；Lane 2：Effluent after supernatant incubating with Ni-IDA；Lane3-6：Elution fractions. (C) SDS-PAGE and Western Blot. Left：SDS-PAGE. Right：Western Blot (using anti-His tag antibody). Lane 1：BSA (1.0 μg)；Lane 2：CD14-Fcε protein (1.2 μg)(Reduced)；Lane 3：CD14-Fcε protein (1.2 μg)(Non-Reduced)；Lane M1: SDS-PAGE Marker；Lane M2: Western Blot Marker.

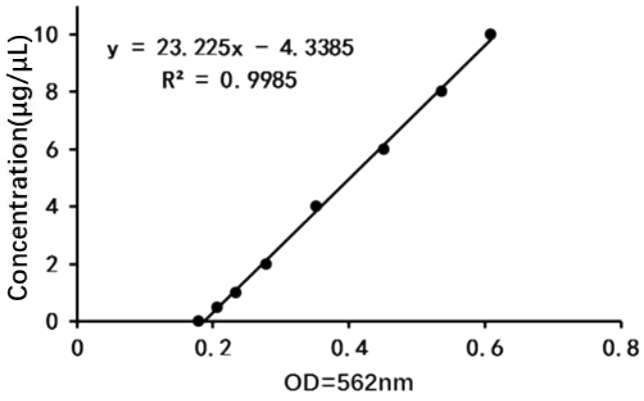

Fig. S4. Standard curve of protein quantification using BCA.

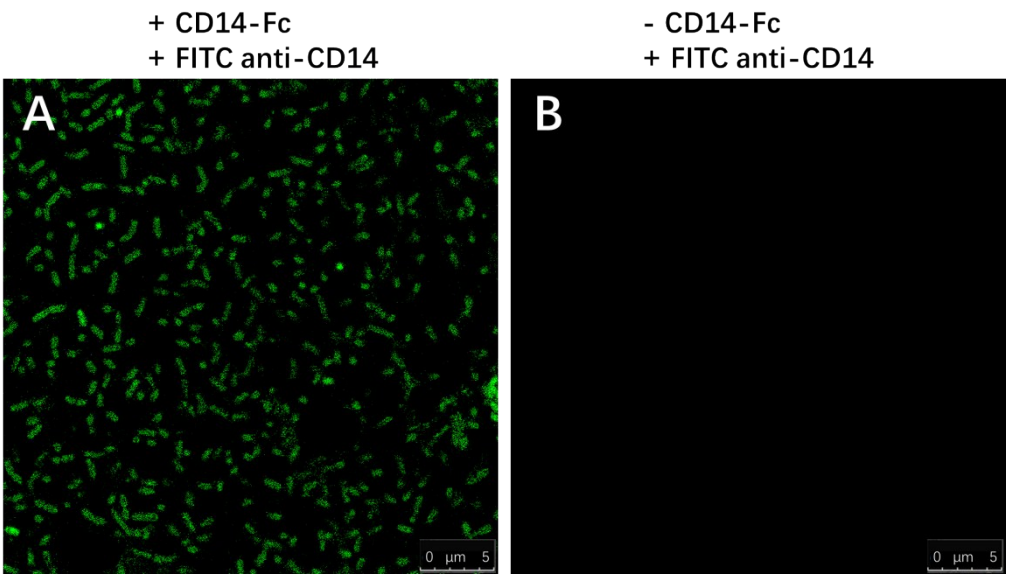

Fig. S5. Immunofluorescence images of CD14-Fcε bound to *E. coli* ATCC 25922. The bacteria were heat-killed and then incubated with (A) or without (B) CD14-Fcε (6 µg/mL) followed by anti-CD14 (2 µg/mL) and IgG-FITC.

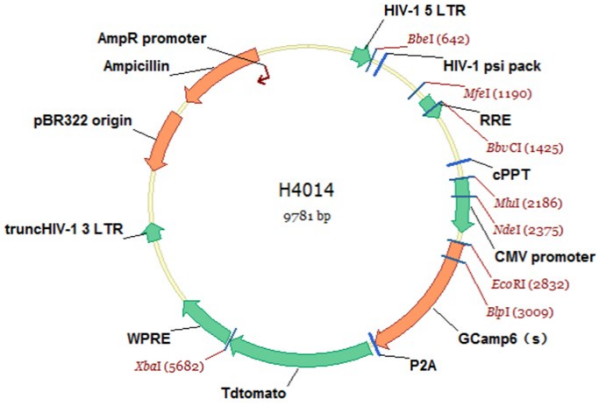

Fig. S6. Plasmid profile of pLenti-CMV-GCaMP6(s)-2A-Tdtomato

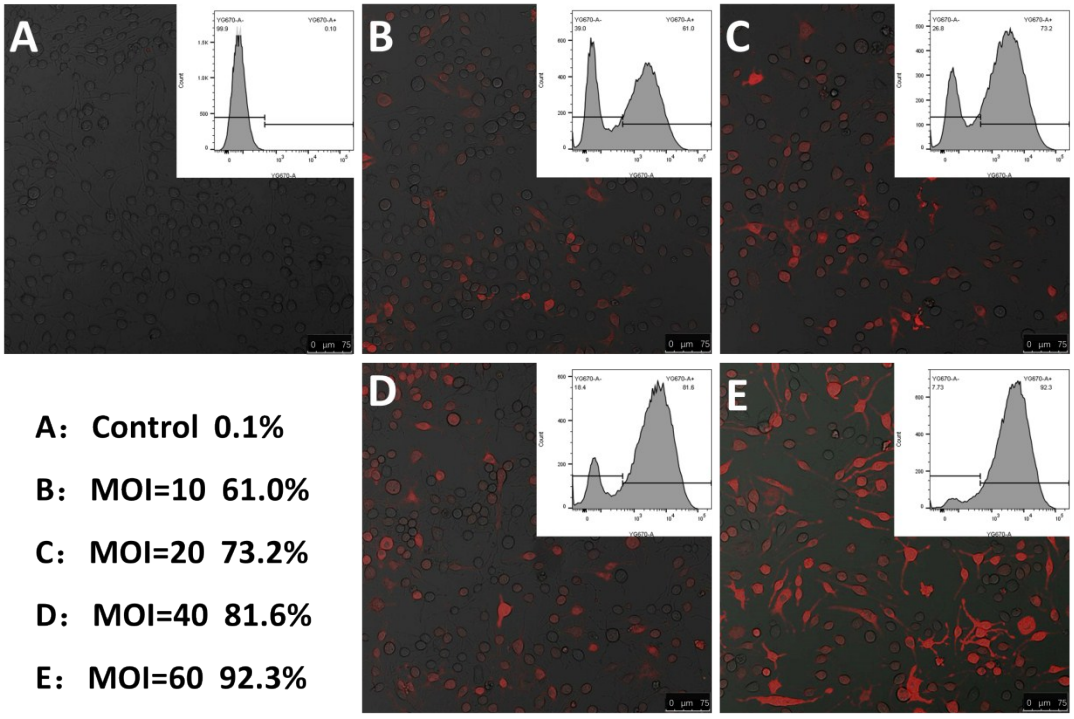

Fig. S7. Lentiviral vector transfection and selection of stable transfection cell lines.

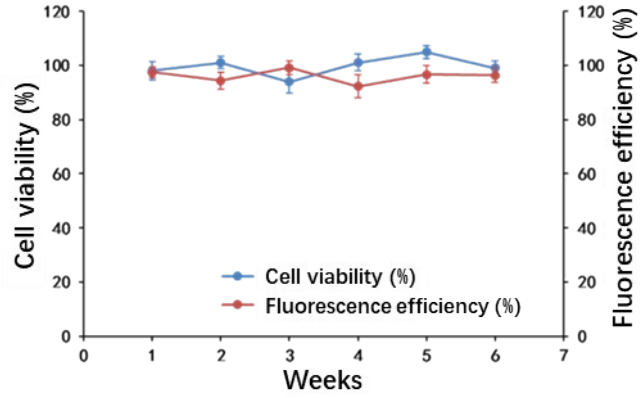

Fig. S8. Cell viability and fluorescence efficiency.

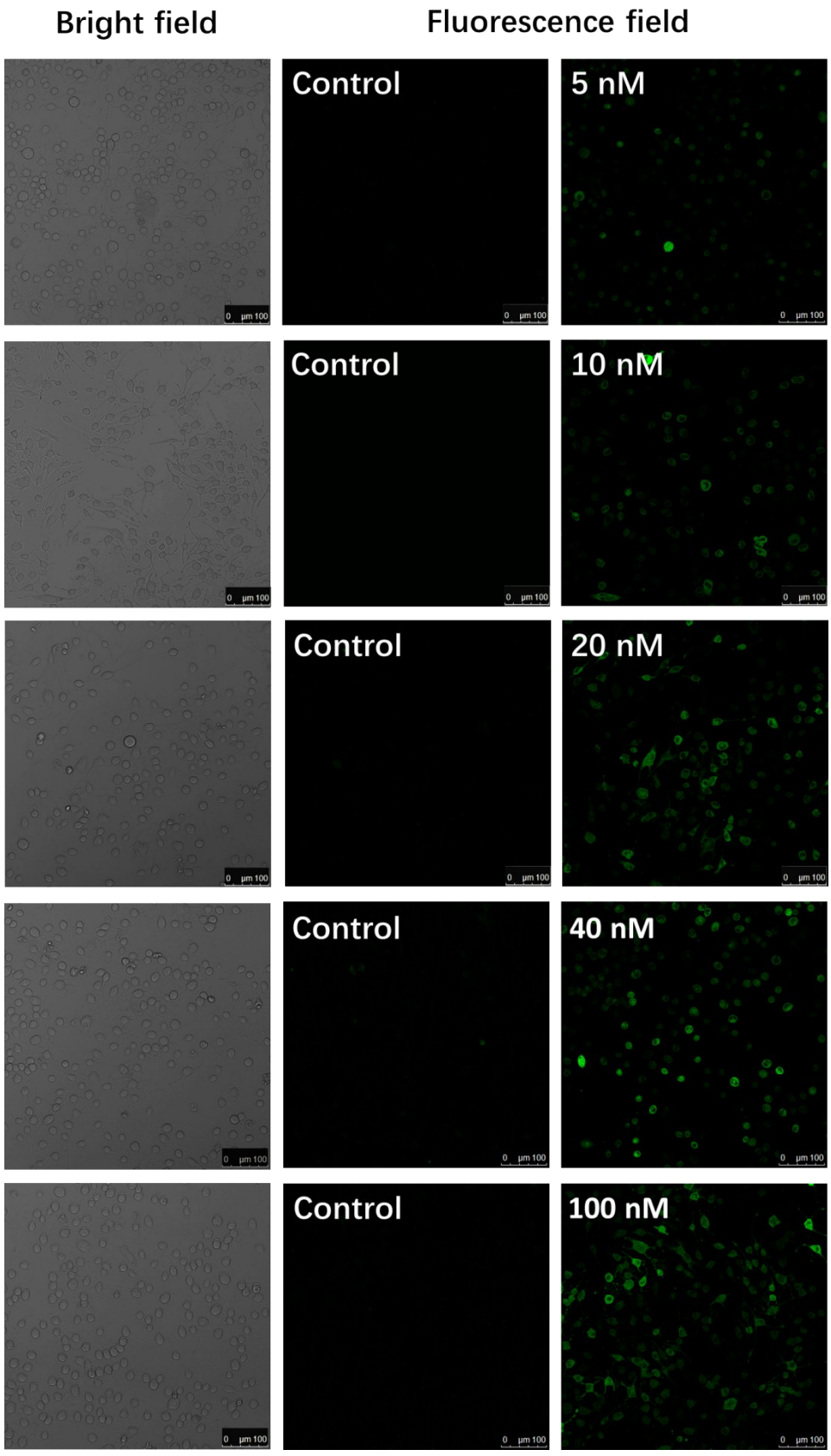

Fig. S9. Fluorescence images of stable transfection RBL-2H3 cell lines after A23187 stimulation.

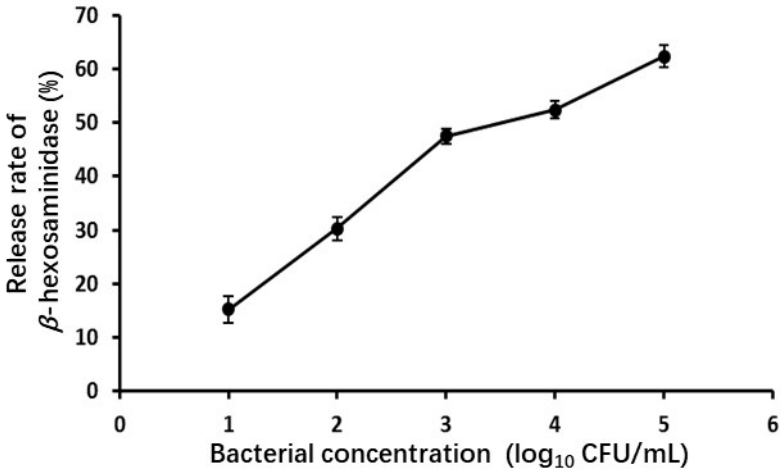

Fig. S10. *β*-hexosaminidase assay for confirmation of RBL-2H3 cells activated by *E.coli* ATCC 25922.

Table S1 Comparison of other methods for bacteria detection.

Target	Detection method	Linear range (CFU/mL)	LOD (CFU/mL)	Detection time	Ref.
E. coli O157:H7.	Impedance based ferrocene-antimicrobial peptide modified biosensor	10^3–10^7	10^3	a couple of hours	(Li et al. 2014)
E. coli O157:H7	Aptamer-based QCM sensor	10^2–10^7	1.46×10^3	1 h	(Yu et al. 2018)
E. coli O157:H7.	Microfluidic colorimetric biosensor	5.0×10^1–5.0×10^4	50	45 min	(Zheng et al. 2019)
E. coli O157:H7	Fluorescent biosensor	10–10^6	14	2 h	(Xue et al. 2018)
E. coli	Automated microfluidic-based electrochemical sensor	10–3.97×10^7	50	8 min	(Altintas et al. 2018)
S. aureus	Aptamer-based hydrogel barcodes	10^2–10^4	100	2.5 h	(Xu et al. 2018)
E. faecalis	Molecularly imprinted nanoparticles based plasmonic sensor	2×10^4–1×10^8	1.05×10^2	15 min	(Erdem et al. 2019)
S. Enteritidis	Gram staining and direct immunoassay	10^3–10^8	800	11 min	(Bu et al. 2019)
V. parahaemolyticus	Aptamer-based visualized detection	10–10^6	10	2 h	(Song et al. 2019)
E. coli & *S. aureus*	Paper-based colorimetric assay	10^4–10^8	10^4	20 min	(Sun et al. 2019)
gram-negative bacteria	FcεRI-IgE-based genetically encoded microfluidic cell sensor	8×10^1–5×10^3	80	2.5 min	This study

References

Altintas, Z., Akgun, M., Kokturk, G., Uludag, Y., 2018. A fully automated microfluidic-based electrochemical sensor for real-time bacteria detection. Biosensors & Bioelectronics 100, 541-548.

Bu, T., Huang, Q., Yan, L., Zhang, W., Dou, L., Huang, L., Yang, Q., Zhao, B., Yang, B., Li, T., Wang, J., Zhang, D., 2019. Applicability of biological dye tracer in strip biosensor for ultrasensitive detection of pathogenic bacteria. Food Chemistry 274, 816-821.

Erdem, O., Saylan, Y., Cihangir, N., Denizli, A., 2019. Molecularly imprinted nanoparticles based plasmonic sensors for real-time Enterococcus faecalis detection. Biosensors & Bioelectronics 126, 608-614.

Li, Y., Afrasiabi, R., Fathi, F., Wang, N., Xiang, C., Love, R., She, Z., Kraatz, H.-B., 2014. Impedance based detection of pathogenic E-coli O157:H7 using a ferrocene-antimicrobial peptide modified biosensor. Biosensors & Bioelectronics 58, 193-199.

Song, S., Wang, X., Xu, K., Xia, G., Yang, X., 2019. Visualized Detection of Vibrio parahaemolyticus in Food Samples Using Dual-Functional Aptamers and Cut-Assisted Rolling Circle Amplification. Journal of Agricultural and Food Chemistry 67(4), 1244-1253.

Sun, J., Huang, J., Li, Y., Lv, J., Ding, X., 2019. A simple and rapid colorimetric bacteria detection method based on bacterial inhibition of glucose oxidase-catalyzed reaction. Talanta 197, 304-309.

Xu, Y., Wang, H., Luan, C., Liu, Y., Chen, B., Zhao, Y., 2018. Aptamer-based hydrogel barcodes for the capture and detection of multiple types of pathogenic bacteria. Biosensors & Bioelectronics 100, 404-410.

Xue, L., Zheng, L., Zhang, H., Jin, X., Lin, J., 2018. An ultrasensitive fluorescent biosensor using high gradient magnetic separation and quantum dots for fast detection of foodborne pathogenic bacteria. Sensors and Actuators B-Chemical 265, 318-325.

Yu, X., Chen, F., Wang, R., Li, Y., 2018. Whole-bacterium SELEX of DNA aptamers for rapid detection of E. coli O157:H7 using a QCM sensor. Journal of Biotechnology 266, 39-49.

Zheng, L., Cai, G., Wang, S., Liao, M., Li, Y., Lin, J., 2019. A microfluidic colorimetric biosensor for rapid detection of Escherichia coli 0157:H7 using gold nanoparticle aggregation and smart phone imaging. Biosensors & Bioelectronics 124, 143-149.